Reduced complexity debris flow/flood hazard assessment at the southwestern slope of Mt. Omo, L'Aquila municipality, central Italy

Luigi Guerriero[a], Mirko Francioni[b*] Domenico Calcaterra[a], Diego Di Martire[a], Simone Palumbo[c], Claudia Zito[c], Nicola Sciarra[c]

[a] Department of Earth, Environmental and Resource Sciences, Federico II University of Naples, Naples, Italy.

[b] Department of Pure and Applied Sciences, University of Urbino Carlo Bo, Urbino, Italy.

[c] Department of Engineering and Geology, University G. d'Annunzio Chieti-Pescara, Chieti, Italy.

Correspondence to: Mirko Francioni, mirko.francioni@uniurb.it

Abstract

In recent decades, the increasing number and severity of wildfires have become a major concern in many regions of the world. Beside direct consequences on forests, crops and settlements, wildfires can have significant effects on catchment's hydrology, altering their response to rainfall and promoting enhanced runoff and erosion. Increased runoff in burnt areas can result in catastrophic damage and loss of life by destructive debris flows and floods. Although observed in many regions of the world, post-wildfire debris flows/floods seem to prevail in western Unites States and southern Europe. In Italy, post-wildfire debris flows/floods have been observed in a number of sectors of the Apennine range and a total of 113 events occurred between 2001 and 2021 in Campania region. A recent event occurred on August 24, 2020, in the *Fosso delle Pescine* catchment, on the southwestern slope of the Mt. Omo in the L'Aquila municipality, hit by a severe wildfire at the beginning of the month. Consequences of the event on people and properties indicate the need for an evaluation of debris flow/flood hazard in both pre- and post-wildfire condition. The analysis of these events may often be complex, requiring time and many input data. In this context, a simplified method of analysis which accounts for event initiation and propagation through a shallow water equation based approach would represent a new an innovative solution for fast and preliminary debris flow/flood analyses. In this research, a reduced complexity analysis based on probability analysis of rainfall and 2D hydrodynamic modeling was carried out by estimating i) wildfire extent and severity, ii) sediment characteristics and availability, iii) potential runoff induced by rainfall and iv) inundation by debris flow/flood. A debris flow/flood hazard model was developed on the basis of multiple return periods (10, 50, 100 and 300 years) debris flow inundation scenarios derived by non-Newtonian 2D hydrodynamic modeling of debris flow hydrograph and qualitatively validated on the basis of extent of alluvial fan deposits. Potential drowbacks of the model are related to the possible overestimation of surface runoff, related to the consideration of the whole catchment contributing area and the limited volumetric sediment budget available at the headwater, which might not sustain high return period event generation. Debris flow/flood event might be originated by rainfall concentrated at the headwater of the catchment.

1. Introduction

In the last decades, the ongoing climate change and the increasing human pressure have been responsible for a change in frequency and magnitude of storms, wildfires, floods and landslides. The incidence of wildfires is consistently growing in many forested regions of the world due to an increased temperature and drought, which extend the wildfire season length (Wieczorek and Bryant, 2008; Williams et al., 2019). Further causes have been identified in an increase in the number of fire ignitions and the effect of fire suppression policies that have led to greater natural fuel availability (Cannon and DeGraff, 2009).

As indicated by Parise and Cannon (2012), wildfire can alter the hydrologic response of a drainage basin by reducing rainfall infiltration and increasing surface runoff. This is caused by the i) removal of soil-mantling vegetation and litter, ii) deposition of ash, iii) change in physical properties of both soil and rock and iv) the enhancement, generation, or destruction of water-repellent soils. These changes have effect also on the attitude of soils to be eroded and sediment availability for mobilization by water flow (Moody and Martin, 2001). As a consequence, combination of sediment-laden flows and debris-flows or/and -floods (i.e. debris-flow/flood; Hungr et al., 2014) can occur after wildfire (Cannon, 2001; w et al., 2001). A number of Authors have analyzed conditions for post-wildfire debris flow and flood development. For instance, Cannon (2001) evaluated the erosional response of a number of burned basins in western United States indicating that only ~40 % of these basins produced debris flows. Cannon interpreted the fact that not all burned basins produced debris flows relating their occurrence to specific geologic and geomorphologic conditions that control post-wildfire debris flow generation (drainage-basin morphology, lithology, etc.). Cannon et al. (2010) estimated relations between rainfall and post-wildfire debris-flow and -flood magnitude in the San Gabriel Mountains of southern California. They indicated that debris flow and floods were triggered as a consequence of storms of duration between 45 minutes and 38 hours and total rainfall between ~13 and ~390 mm.

Post-wildfire debris flows can be initiated by both infiltration-triggered soil slip or runoff-dominated erosion and sediment entrainment into the surface flow (Parise and Cannon, 2012). Although both mechanisms have been documented, it seems that channel erosion and scour are the dominant sources of debris in many burned areas of the western United States, with yield rates increasing significantly partway down the channel (Santi et al., 2008). Church and Jakob (2020) identified multiple triggering mechanism for debris floods but, in burned basins, they can be initiated by runoff-dominated erosion or debris-flow dilution. For surface-runoff initiated debris-flows and -floods, the timing and magnitude of all events are consistently associated with local peaks in short duration rainfall and channel response in terms of flow stage is very fast (few minutes to few hours, Kean et al., 2011; Borga et al., 2014). Staley et al. (2013) determined that hillslope-divergent and hillslope-convergent process domains represent the primary sources of material in southern California and concluded that raindrop-impact induced erosion, ravel, surface wash, and rilling are the primary erosional processes contributing to post-wildfire debris-flow initiation.

Although observed in many regions of the world, post-wildfire debris flows and floods seem to prevail in western Unites States and southern Europe. For instance, in Colorado (USA), the South Canyon Fire of July 1994 burned 800 ha of vegetation on Storm King Mountain near Glenwood Springs. Two months later debris flows occurred in response to torrential rains, inundating areas along a 5-km length of Interstate Highway 70 (Cannon et al., 1998). In southwestern Montana, in the fall of 2001, an intense thunderstorm triggered many debris-flows and -floods in the burned area of Sleeping Child Creek (Gabet and Bookter, 2008). In California, immediately after the 2003 Grand Prix wildfire near San Bernardino, a large winter rainstorm on December 24–25, 2003, produced numerous debris-flows and -floods in many of the burned drainage basins and resulted in 16 fatalities and millions of dollars in damage (U.S. Army Corps of Engineers 2005). In Spain, debris flows triggered by a brief and intense rainfall occurred three weeks after a wildfire in August 1986 in the Najerilla River valley in the Iberian Range. In Italy, post-wildfire debris flows have been observed in a number of sectors of the Apennine range (Calcaterra et al., 2007; Carabella et al., 2019; Di Napoli et al., 2020; Esposito et al., 2022).

On August 24, 2020, a combined debris-flow and -flood (e.g. Cannon 2001) occurred in the so-called *Fosso delle Pescine* catchment, on the southwestern slope of the Mount Omo in the L'Aquila municipality, hit by a severe wildfire at the beginning of the month. Consequences of the event on people

and properties indicate the need for an evaluation of hazard in both pre- and post-wildfire conditions for the catchment and the adjacent village of *Arischia*. In this perspective, conditions of development of the August 24 event were considered as a reference scenario, so that an initial assessment of the area affected by the wildfire in terms of extent and severity was carried out on the basis of multispectral satellite data. Subsequently, sediment characteristics and availability after the event was evaluated by field surveys and such data were used as a basis for debris flow 2D hydrodynamic modeling. Rainfall data of the L'Aquila meteorological station were used for probabilistic estimation of potential runoff by Soil Conservation Service (SCS) method. Throughout the text the term debris-flow/flood is consistently used to describe the phenomenon object of analysis because, according to characteristics of the August 24 event, model parameterization was carried out considering a parametric scenario supporting both debris-flow and -flood prediction. Similarly, Destro et al. (2018) completed a coupled prediction of flash flood response and debris flow occurrence in the Alpine environment using a distributed hydrological model.

2. Study area

The study area is located in the upper sector of the middle *Aterno* river valley in the Apennine Mountains of central Italy, next to the L'Aquila-Coppito plain. It comprises the *Fosso delle Pescine* catchment (northern sector of the area), developed along the southwestern slope of the Mt. Omo, and the adjacent village of *Arischia* (southern sector of the area), both affected by the August 24, 2020, debris flow event (Fig. 1). From a geological point of view, the northern sector of the study area is characterized by the presence of Mesozoic carbonate rocks forming Mt. Omo, locally cataclasized and/or covered by recent slope and colluvial deposits. Downslope, the *Arischia* village develops at the margin of the L'Aquila-Coppito plain, along the northeastern side of the *Aterno* river valley next to the confluence with the *Fosso del Ferone*. In this area, slope and terraced alluvial deposits are associated with significantly developed and active debris fans. The L'Aquila-Coppito plain corresponds to a tectonic sub-basin (belonging to the L'Aquila tectonic basin) bounded by NW-SE trending normal faults and fault systems. Such tectonic structures, which follow the general Apennine trend, are the most common in the study area but local NE-SW trending trans-tensive faults are also present. The morphology of the study area is the result of a long-term evolution responsible for the development of structural, fluvial and karst landforms (Santo et al., 2013). Its northern sector is dominated by structural landforms such as triangular facets and saddles characterizing the southwestern slope of the Mt. Omo. The *Fosso delle Pescine* channel crosses this slope in a longitudinal manner and its valley is characterized by an asymmetric cross-sectional shape with its right flank significantly more inclined than its left flank. This asymmetry is potentially related to the different degree of damage of the carbonate rocks forming the slope bedrock, which crops out as a cataclasized rock mainly along the right side of the valley. The transition area between Mt. Omo slope and the L'Aquila-Coppito plain is characterized by the presence of multiple active debris fans, locally covering multiple-order fluvial terraces. Both landforms characterize the southern sector of the study area.

The debris flow/flood event of August 24, 2020, developed as a consequence of a high duration and intensity rainfall event, reached the Arischia village. Although several landslide scars were observed along the right side of the *Fosso delle Pescine* channel, the event potentially initiated as debris flow at the headwater of the catchment by sediment entrainment into the surface water flow due to runoff-dominated erosion, and subsequently transformed into debris flood through dilution by tributary water-ash flow mixture. Indeed, the Arischia village was affected by a debris flood. In this area, significant outcrops of cataclasized rocks with a limited thickness of mobilizable sediment, representing a significant source of sediment for debris flow development, were observed. Observations of signs of abrasion on tree stems along the channel indicated that the depth of the flow during the event consistently grew downslope with a maximum thickness of ~1 m in the lower segment of the bedrock channel.

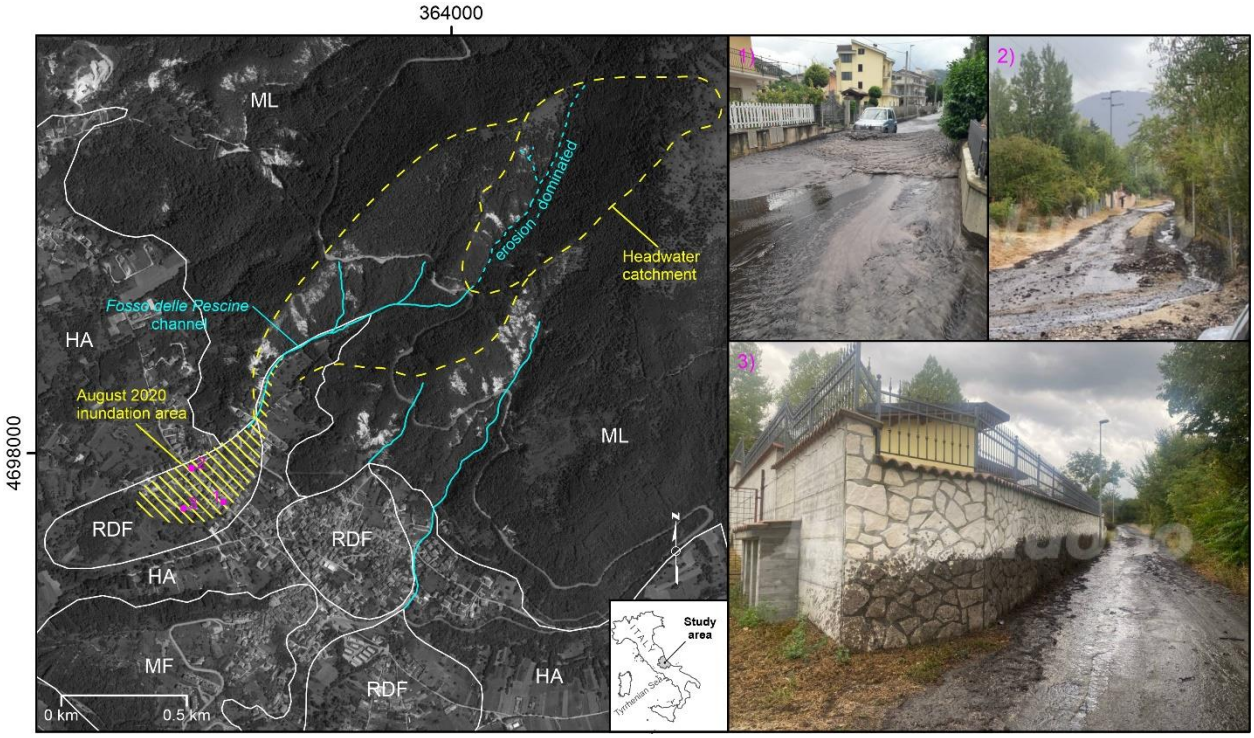

Figure 1 – Map showing major geological features of the area as well as the Fosso delle Pescine catchment, its headwater catchment, and the reconstructed shape of the area inundated by the August 2020 event. Legend: ML, Mesozoic limestones; MF, Miocene Flyschoid deposits; HA, Holocene alluvial deposits; RFD, Recent Alluvial Fan. The Figure also highlights photographs of the 2020 event and the location on the map from where the photographs were taken (Photographs source: 1) https://www.laquilablog.it/; 2) e 3) https://www.ilcapoluogo.it/.

3. Materials and methods

3.1 Materials

The analysis of residual debris-flow/flood hazard in the *Fosso delle Pescine* catchment – *Arischia* village area was carried out based on a variety of available materials. Sentinel-2 L2A high-resolution and multispectral satellite images were used as a basis for the assessment of the area affected by the wildfire in terms of extent and severity, which had to be considered in runoff modeling. Sentinel 2 products are acquired by satellites equipped with a multispectral detector (MultiSpectral Instrument, MSI) able to sample 13 spectral bands with different Ground Sampling Distance (GSD): RGB-NIR bands - 10 m, VREs-SWIR bands - 20 m, and Coastal aerosol-Water vapor -Cirrus bands - 60 m. Due to the need of correctly identifying the signature of the wildfire, a pre-event and a post-event Sentinel 2 image, acquired on 29/07/2020 and 03/08/2020, respectively, were used for the analysis. The first image represents the pre-wildfire condition of the affected catchment. A 1:5000 numerical cartography (*Carta Tecnica Regionale*), produced by the Abruzzo region, was used as a basis for field surveys. A 10 × 10 m Digital Elevation Model (DEM) produced by Tarquini et al., (2007) was associated to the numerical cartography and used as a support for field surveys, for catchment morphometric analysis and 2D hydrodynamic modeling of debris flow/flood initiation and propagation. For probabilistic runoff estimation, rainfall data characterized by significant length and continuity of records, in the form of annual maxima, were derived for specific durations (1, 3, 6, 12 and 24 hours) by the time series acquired from the L'Aquila meteorological station between 1933 and 2010. The meteorological station was located few kilometers south of the study area at 685 m above the sea level (asl).

3.2 Methods

The analysis of residual debris flow/flood hazard in the Fosso delle Pescine catchment and the Arischia village was completed through a multi-method approach (Fig. 2) considering the post August 2020-event conditions as a reference scenario for the assessment. Since the event occurred after a wildfire, an initial evaluation of the extent and severity of the burned areas of the *Fosso delle Pescine* catchment was carried out based on well-known spectral indices, estimated using available pre- and post-wildfire multispectral satellite imagery. Obtained distribution of burned areas and estimated severity were considered for runoff modeling through the SCS method. Field surveys were carried out over the catchment area to estimate thickness of sediment, available for debris flow/flood initiation, and took samples for laboratory analysis. Grain size distribution and unit weight were determined on remolded samples taken along and next to the *Fosso delle Pescine* channel. Volumetric sediment availability and sediment characteristics were subsequently considered in 2D hydrodynamic modeling of debris flow/flood to validate modeling hypothesis (e.g. potential sediment concentration, shear strength, etc…).

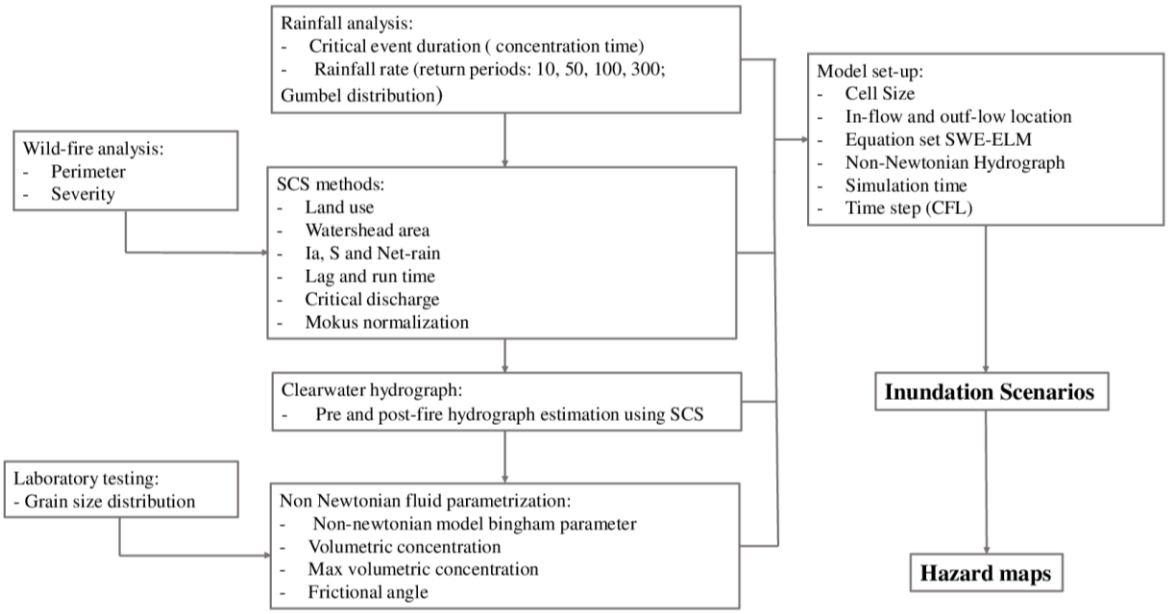

Figure 2 – Flow chart showing methodological framework used for debris flow hazard assessment.

3.2.1 Wildfire analysis

The wildfire was analyzed in terms of extent and severity using the Normalized Burning Ratio and the Normalized Burning Ratio 2 (NBR and NBR 2; Roy et al., 2006). These indices use near infrared (NIR) and short wave infrared (SWIR) bands to derive a burning index suitable for the identification of burned areas and the measure of burn severity. Since healthy vegetation shows high reflectance in the NIR and low reflectance in the SWIR, while burned areas have high reflectance in SWIR and low in NIR, NBR index allows to identify burned and non-burned area through the following function:

$$NBR = (NIR-SWIR)/(NIR+SWIR) \quad (1)$$

where NIR and SWIR represents the Bottom of the Atmosphere (BoA) reflectance in the near (NIR, B08) and in the short wave infrared band (SWIR, B11), respectively. In comparison with the Normalized Burning Ratio (NBR), the Normalized Burning Ratio 2 (NBR 2), highlighting the water sensitivity in vegetation, has better performance in wildfire severity estimation, and has therefore been used at this

purpose. This index uses two SWIR spectral bands (B11 and B12) to identify burn severity and has the following form:

$$NBR2 = (SWIR1-SWIR2)/(SWIR1+SWIR2) \quad (2)$$

where SWIR1 and SWIR2 represents the BoA reflectance in the short wave infrared band 1 and 2 (B11 and B12). For a better estimation of wildfire severity, a relative approach based on a delta Normalized Burning Ratios dNBRs (e.g. Miller and Thode, 2007), commonly used in change detection analysis, was adopted. Wildfire extent was derived from the difference between the NBR2 before and the NBR2 after the wildfire, calculated as follows:

$$dNBR2 = (NBR2 \text{ pre fire})-(NBR2 \text{ post fire}) \quad (3)$$

Wildfire extent and maximum severity scenario were considered for the subsequent modeling of surface runoff through the SCS method (SCS, 1972).

3.2.2 Field survey and laboratory testing

Sediment availability for debris flow/flood initiation and grain size distribution characteristics were assessed by field surveys and laboratory testing. Local measurements of sediment thickness were carried out in the field using a low diameter steel rod. The rod was pushed by hand in the superficial deposit and penetration depth was measured. Such depth was assumed to correspond to easily mobilized sediment thickness. Measurement locations were selected based on local accessibility and morphology. Especially, a series of punctual measurements were carried out along cross-sectional profiles selected at different elevation of the channel (Fig. 3). Further measurements were completed at locations considered significant to the analysis. Soil thickness measurements were subsequently used to create a sediment thickness model of the catchment by polynomial interpolation of data as function of slope and elevation. Overall volumetric sediment availability was than estimated. For grain size distribution analysis, several soil samples were taken at different elevation along the channel and at significant locations (Fig. 3). Soil samples were analyzed following the ASTM D 421 method. The derived volumetric sediment availability and grain size distribution curves were subsequently considered in 2D hydrodynamic modeling.

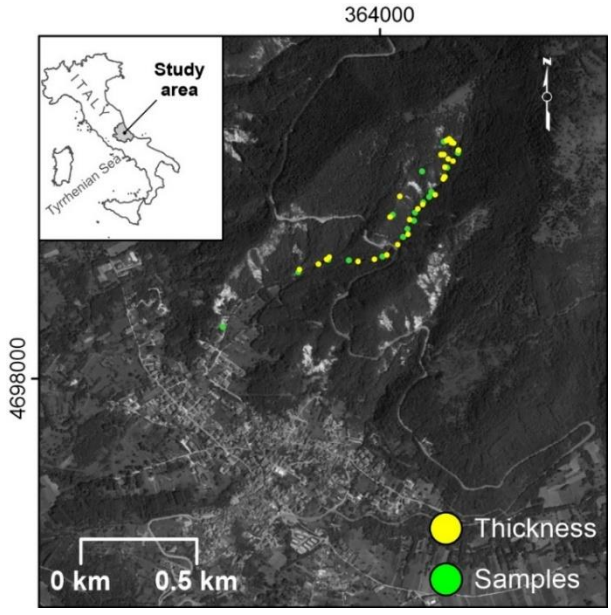

Figure 3 – a) Map showing position of sediment thickness measures and sampling locations.

With regards to the soil type and land use/cover, these were derived combining an extensive field survey and orthophotos analysis and subsequently used to extract the absorption ratio through the SCS-CN (SCS, 1972) associate literature.

3.2.3 Rainfall analysis and runoff estimation

Debris flow/flood hazard assessment was carried out considering runoff potential evaluated based on Intensity-Duration-Frequency (IDF) curves. To derive these curves, form the available annual maxima time series, probability of rainfall was estimated by fitting annual maxima data using a type I Generalized Extreme Value (GEV) distribution (Gumbel; e.g. Jenkinson, 1955) in the form of a Cumulative Distribution Function (CDF). The probability function F(h) is expressed as:

$$F\ (h) = \exp\ \{ -\exp\ [-\ (\alpha\ (h\ -\ \mathrm{u})]\}\ (1)$$

where h is the maxima rainfall height, the parameters α and u are estimated considering the mean value of the series (μ) and its standard deviation (σ) through the following equations:

$$\alpha = \frac{1.283}{\sigma}\ (2)$$

$$u = \mu - 0.45\ \sigma\ (3).$$

F(h) represents the probability of not exceeding the value of the rainfall height h by that random variable. Fixed the return period, with T >1, the inverse of the CDF (i.e. a survivor distribution function) provides the values of h on the basis of return period T and duration d:

$$h(d) = u(d) - \frac{1}{\alpha(d)}\ln(-\ln(1 - \frac{1}{T}))\ (4).$$

The equation (4) allows to define the height-duration-frequency curves, generally described by the expression:

$$h(d,T) = a\ (T)d^n\ (5)$$

in which a and n are parameters estimated through graphical or probabilistic approach. Subsequently, the height-duration-frequency curves were transformed in IDF curves. According to the guidelines of the local competent authority (*Autorità dei Bacini di Rilievo Regionale dell'Abruzzo e del Bacino Interregionale del Fiume Sangro*), the return period considered for debris flow hazard analysis were: (i) 10-years, (ii) 50-years, (iii) 100-years and (iv) 300-years. The obtained IDF curves were subsequently used for runoff estimation through clear water synthetic unit hydrograph reconstruction using the SCS-CN method (SCS, 1972). The synthetic unit hydrograph is expressed as the ratio of runoff Q and peak of discharge Q_p, and the ratio of time t (duration of rainfall) and time to peak t_a (Ramírez, 2000). The Q/Q_p ratio increases over time and reaches a maximum value (equal to 1) when Q equals Q_p. Subsequently, it decreases until it reaches a value near zero. The time required to reach the peak and return to zero defines the duration of the hydrograph. The SCS-CN method is based on the equation:

$$\frac{P\ -\ I_a\ -\ Q}{S} = \frac{Q}{P - I_a}\ (6)$$

where P is the cumulative rainfall (mm), I_a the initial abstraction (mm), Q the runoff and S the potential maximum soil moisture retention after runoff initiation (mm). Respect to the runoff, Eq. (6) takes the form:

$$Q = \frac{(P - I_a)^2}{(P - I_a) + S} \quad (7).$$

Eq. (7) is used to obtaining predictions of Q using just a few input variables. Further simplifications of the SCS-CN method are represented by the average value for I_a, selected as 0.2 S and by the introduction of the Curve Number (CN) that allow to estimate S as:

$$S = \left(\frac{25400 - 254\,CN}{CN}\right) (8).$$

CN varies between 30 for low runoff potential (and high infiltration) and 100 for high runoff potential, depending on land use, hydrologic soil group, hydrologic condition, and Antecedent Moisture Conditions (AMC) (SCS, 1972). In this case, after estimating CN for the different types of soils (based on land use classes), CN post-fire has been evaluated based on CN pre-fire and fire severity with weighted values of 80 for pre-fire condition and 92 in post-fire ones. In this way, pre- and post-wildfire net hyetographs representing surface runoff over the *Fosso delle Pescine* catchment, were reconstructed.

In this analysis, clear water Synthetic unit hydrograph were simplified as triangular and, considering the limited size of the catchment, timing parameter were evaluated using the SCS lag equation. The ascending and descending phases account for a specific duration represented by the accumulation time t_a. Considering that Q (7) corresponds to the net rainfall P_n, the peak discharge was obtained through the equation:

$$Q_p = 0.278 \frac{P_n A}{t_a} \quad (9)$$

where A is the area of the catchment and t_a is the accumulation time. Concentration time t_c was estimated using the Ventura's formulation. Synthetic unit hydrographs were then used to develop clear water runoff hydrographs on the basis of cumulative rainfall derived by IDF curves.

With the goal of refining the SCS-CN parameters, a trial and error calibration routine was carried out until the simulation results were coherent with field observation data, and in particular with the observations of signs of abrasion on tree stems along the channel and existing geological maps.

3.2.4 Debris flow/flood inundation modeling and hazard mapping

Debris flow/flood hazard mapping was carried out on the basis of inundation scenarios produced considering clear water hydrographs, corresponding to different return periods (10, 50, 100 and 300 years), and sediment concentration at transition between debris-flow and -flood. Inundation scenario simulations were completed in HEC-RAS environment using the diffusion wave equations and the DebrisLib (Gibson et al., 2020) numerical library framework, developed to simulate non-Newtonian geophysical flows. The diffusion wave equations method was selected because of its modeling ability of flow along steep channel and its computational stability. These equations simulate the flow as strictly driven by gravity and friction (local and convective acceleration are not considered), so that super elevation and local velocity variations cannot be well predicted. These limitations are consistent with the reduced complexity of the selected hazard assessment approach that well apply to the not so complex geometry of the *Fosso delle Pescine* channel. DebrisLib includes a wide variety of single-phase non-Newtonian approaches. Among them, being applicable to sediment-laden and debris flow simulation (Major and Pierson, 1992), the Bingham Plastic was considered in this study despite its limitations (Iverson, 1997). This model allows to quantify the internal momentum losses due to solid phase interactions with a simple, linear model with a non-zero intercept:

$$\tau_{MD} = \tau_y + \mu(\dot{y}) \quad (10)$$

where τ_y is the yield strength, namely the shear stress below which the mixture has enough internal strength to resist motion, and μ is the viscosity of the mixture. Both parameters are defined considering the Coulomb formulation implemented in DebriLib and the internal friction angle of the mixture, estimated in 30°. According to Pierson and Costa (1972), a solid volumetric concentration of 50% was considered. Debris flow/flood inundation modeling was based on the 10 × 10 m DEM (from which the software automatically extracts the slope gradient) and inflow assigned to a specific location of the channel, corresponding to the transition between erosion-dominated and deposition-dominated sectors of the catchment (Fig. 1).

After obtained, pre- and post-wildfire inundation scenarios were assembled through ordered overlay (from the most to the least probable) and classified assigning to each inundation area the corresponding return period. In this way pre- and post-wildfire debris flow/flood hazard maps were derived.

4. Results and discussions

4.1. Extent and severity of the burned area

The extent of burned areas were derived from NBR2 analysis. Figures 4a and b show the NBR2 pre- and post-wildfire extracted maps, respectively. Extent of burned areas is represented in the post-fire image of Figure 4b by dark colors. Overall, along the southwestern slope of Mt. Omo, an area of 2.6 Km^2 was affected by the wildifire between July 29th and August 3rd, 2020. The severity of burned areas was extracted by the dNBR2 analysis (Fig. 4c). Following the Key and Benson (2006) criteria, four severity classes were identified based on dNBR2 values. Non-burned areas are represented by dNBR values ranging between -0,333 and 0,099, while low, moderate and high severity areas by dNBR values ranging between 0.100 and 0.269, 0.270 and 0.659 and 0.660 and 1.300, respectively.

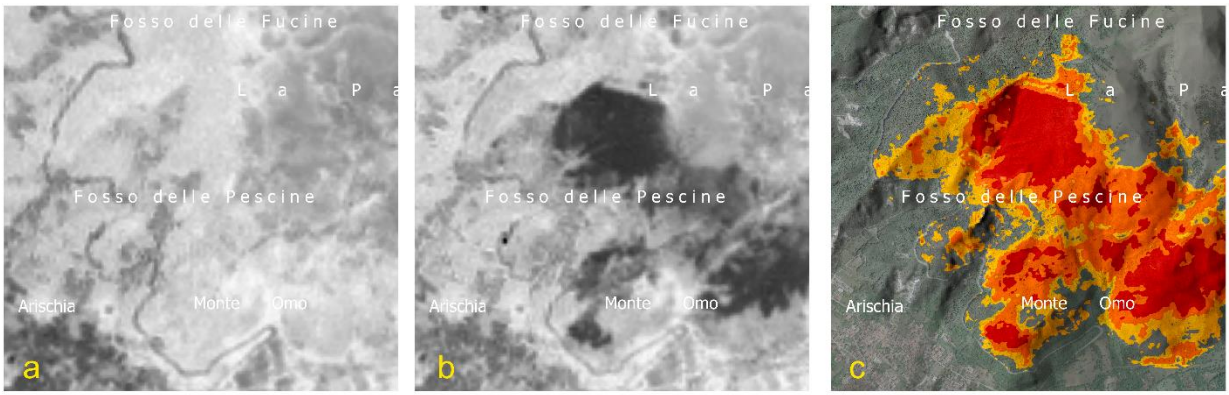

Figure 4 – a) NBR2 pre-fire map; b) NBR2 post-fire map, dark gray color depicts burned areas; c) dNBR2-derived wildfire severity map.

4.2. Surface sediment characteristics

Soil thickness and characteristics have been defined through field survey and particle size distribution laboratory tests. The sampled materials are mainly composed of gravel and sand, with gravel being the main component. Figure 5 shows the particle size distribution curve gathered from 15 samples. Soil thickness values, estimated through field surveys, resulted to be ca 0.8 m and 0.5 along the river bed and

valley sides, respectively. For the headwater of the *Fosso delle Pescine* catchment, a potential volumetric sediment budget higher than 100000 m^3 has been estimated.

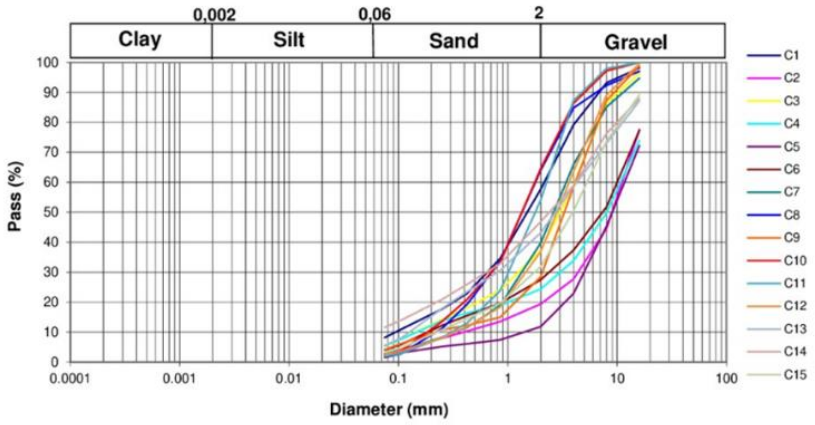

Figure 5 – Particle size distribution of samples taken along the Fosso delle Pescine channel.

It is important to highlight that the sediment budget in this study area is sustained by the present of a complex structural setting, inducing a continue sediment production in the catchment area (i.e. Cataclasite rocks – see Section 2. Study area). This can sustain low to high return period debris flow events. On this basis, also in case of low to high return period debris flow/flood events, sediment budget does not play a key role in term of debris flow/flood magnitude, due to the expected highly continuous sediment availability.

4.3. Probability of rainfall and runoff hydrographs

Figure 6a provides an overview of IDF curves obtained by rainfall analysis for selected return periods. For a critical rainfall duration of 1 h, the maximum intensity ranges between ~30 mm/h of a 10 years event to ~50 mm/h of a 300 years event. The minimum intensity, evaluated for a critical duration of 24 h, varies between ~2.5 mm/h of a 10 years event and ~3.75 mm/h of a 300 years event. Considering that the concentration time t_c was estimated in ~3 h, the calculated amount of rainfall ranges between ~38 mm and ~61 mm as function of the reference return period (i.e. 10 to 300 years). As well, the net rainfall Q ranges between ~8 mm and ~21 mm, in pre-wildfire conditions, and ~20 mm and ~40 mm, in post-wildfire conditions. These estimates were used for the evaluation of Q_p: it varies between ~6 m^3/s and ~18 m^3/s, in pre-wildfire conditions, and ~8 m^3/s and ~22 m^3/s, in post-wildfire conditions. Figure 6b depicts runoff hydrographs developed on the basis of these data and lag time t_l and accumulation time t_a.

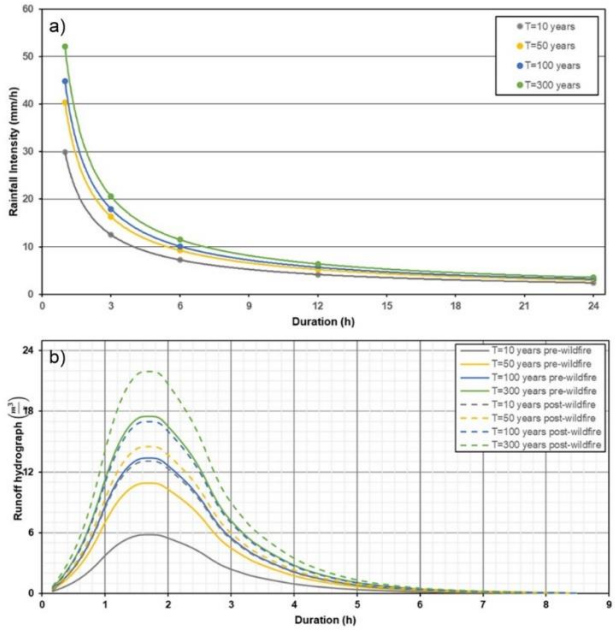

Figure 6 – a) IDF curves developed from the time series registered from the L'Aquila station; b) runoff hydrographs representing potential clear water flow in the lower sector of the Fosso delle Pescine catchment.

4.4. Debris flow propagation scenarios and hazard maps

The data gathered from field and laboratory tests, rainfall and runoff hydrographs and remote sensing extracted maps were used for simulating debris flow/flood propagation scenarios and create hazard maps. The simulations were performed considering pre- and post-wildfire conditions. The return periods contemplated during the analysis were: (i) 10-years, (ii) 50-years, (iii) 100-years and (iv) 300-years.

Figures 7 and 8 show the results of simulations in term of flow velocity and flow depth, respectively. Velocity of flow resulted in pre- and post-wildfire conditions locally higher than 10 m/s, typical of debris flow/flood (Pierson and Costa 1987; Iverson, 2000). Flow-thickness gathered from the simulations ranges from few centimeters up to 2 m. As indicated in the graph of Figure 9, for each scenario, maximum velocity and flow thickness are consistently correlated among them and correlated with the peak of discharge estimated using rainfall data and the SCS-CN method. In the study of debris flow, the balance between potential volumetric sediment budget and rainfalls has to be considered (sediment concentration of 50 % represents the transition condition between debris floods induced by debris flow dilution and debris flows). In fact, the susceptibility to debris flows and their magnitude (i.e. volume) are consistently related to sediment availability (Dong et al., 2009). In this case, a potential volumetric sediment budget higher than 100000 m^3 has been estimated (Section 4.2). In a single event perspective, this budget would sustain the formation of a debris flow mainly for rainfall events of low return period (ca. 10-years). In case of higher return period rainfall events (> 10-years), the higher volume of clear volume and lower sediment concentration generate hyperconcentrated flows (Pierson and Costa, 1987), and/or flood. Having said that, we cannot exclude the formation of events of higher magnitude associated to rainfall of higher return period characterized by a larger extent in terms of involved area. The adopted reduced complexity modeling approach that considers modeling parameter at transition between debris-flow and -flood makes inundation scenarios more representative for this case study and in the different return periods, increasing the reliability of hazard estimation. It is however to be noted that local overestimation of inundation area is possible in case of low return period events. For a better prediction of both phenomena, more complex

approaches able to consider multiple flow regimes have been recently developed (e.g. Jakob et al., 2022). In this research, a first attempt to validate the results have been carried out by comparing flow thickness simulation maps and external morphology of trees impacted by debris flows/flood (Fig. 10). A good correspondence between simulations results and measurements taken on the field has been found, proving the reliability of the models.

Inundation maps were subsequently merged to create a pre- and post-wildfire debris flow/flood hazard map. The extent of each inundation area was classified in relation to the corresponding return period. Very high hazard areas (red) correspond to 10 years return period, high hazard area (orange) to 50 years return period, moderate hazard area (yellow) to 100 years return period and low hazard areas (green) to 300 years return period. Figure 10a and b show the pre- and post-wildfire debris flow/flood hazard map obtained by this procedure. As observable, the area affectable by a post-wildfire events of specific return period is generally larger than that affectable by pre-wildfire events of the same return period. Similarly, a higher flow depth and velocity is expected for post-wildfire events in comparison to pre-wildfire events characterized by the same return period. An explanation for this has to be found in the effect on wildfire on the hydrological and ecological setting of a slope. As indicated by Parise and Cannon (2012), wildfire can alter the hydrologic response of a drainage basin by reducing rainfall infiltration and increasing surface runoff. On this basis and considering the relationship of Figure 9, it appears that after wildfire the study area can be subject to a magnitude enhanced debris flow/flood events. This kind of altered hydrological response might also favor the onset of debris flows in small catchments. The hazard analysis of debris flow/flood involves the estimation of magnitude and frequency in relation to potential triggering rainfall events (Hungr et al., 2005). The adopted reduced complexity approach allows to estimate the magnitude in terms of inundation extent and the frequency in terms of event return period. In general, magnitude and frequency estimation should be completed on the basis of a mid-to-long term record of events that could be developed on the basis of historical records, monitoring data, field surveys, tree-ring analysis, etc. (van Steijn, 1996; Helsen et al., 2002; Hungr et al., 2008; Stoffel, 2010). In this study, due to the absence of such data, an estimation from statistical and physics modeling of surrogate data such as rainfall event have been used according to the studies carried out by Staley et al. (2020).

A further validation of the analysis has been performed by overlaying the hazard maps with the extent of the fan deposit (extracted from the geological map of Figure 1a) and the photographs locations of the 2020 event (location 1, 2 and 3 in Figure 1). A good correspondence has been found between hazard scenario and data from geological map and photographs locations, thus demonstrating the reliability of the simulations.

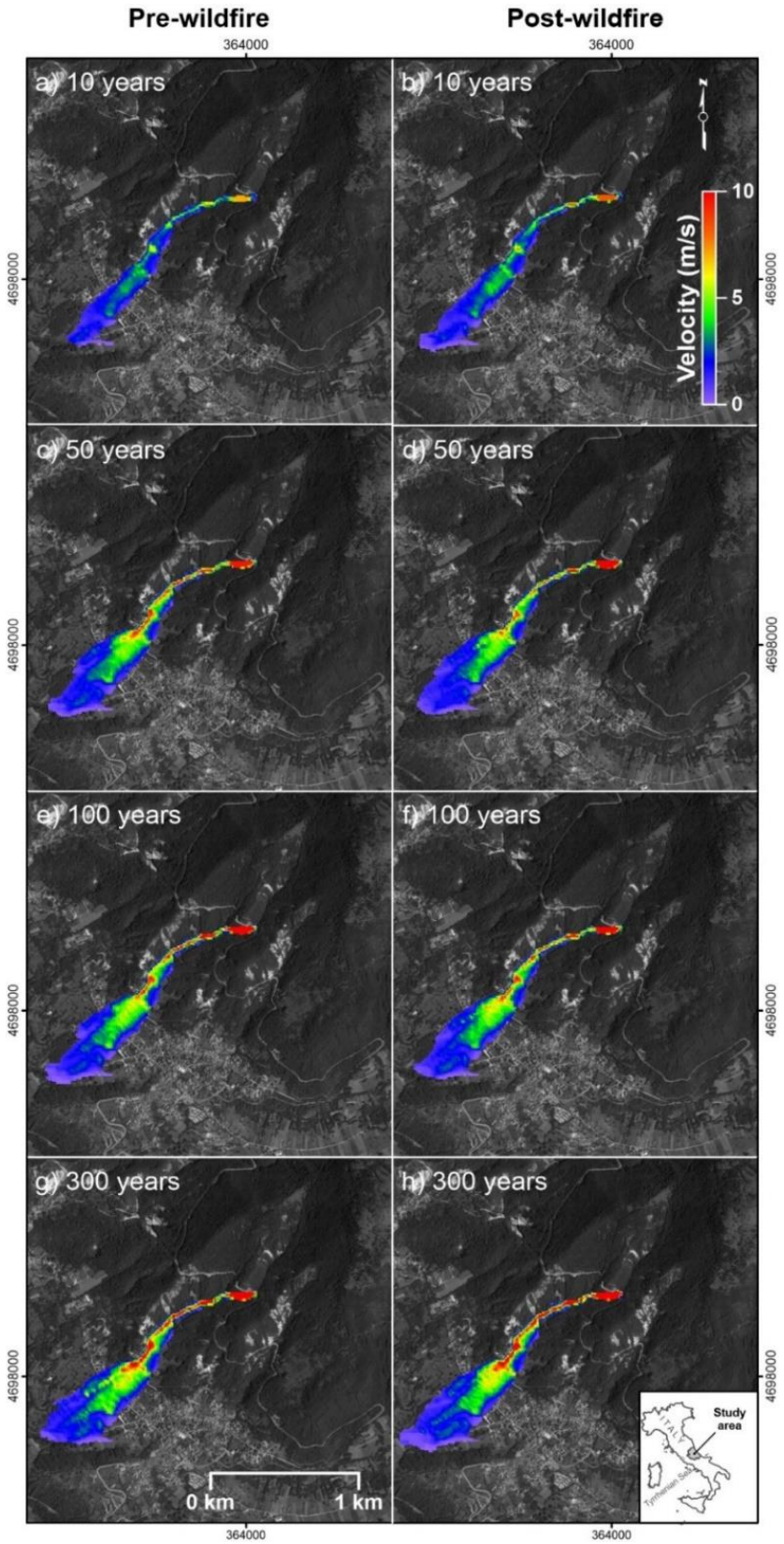

Figure 7 – Pre- and post-wildfire flow velocity scenarios derived from 2D hydrodynamic modeling. For a better visualization of results, the maximum value of the velocity scale is fixed to 10 m/s.

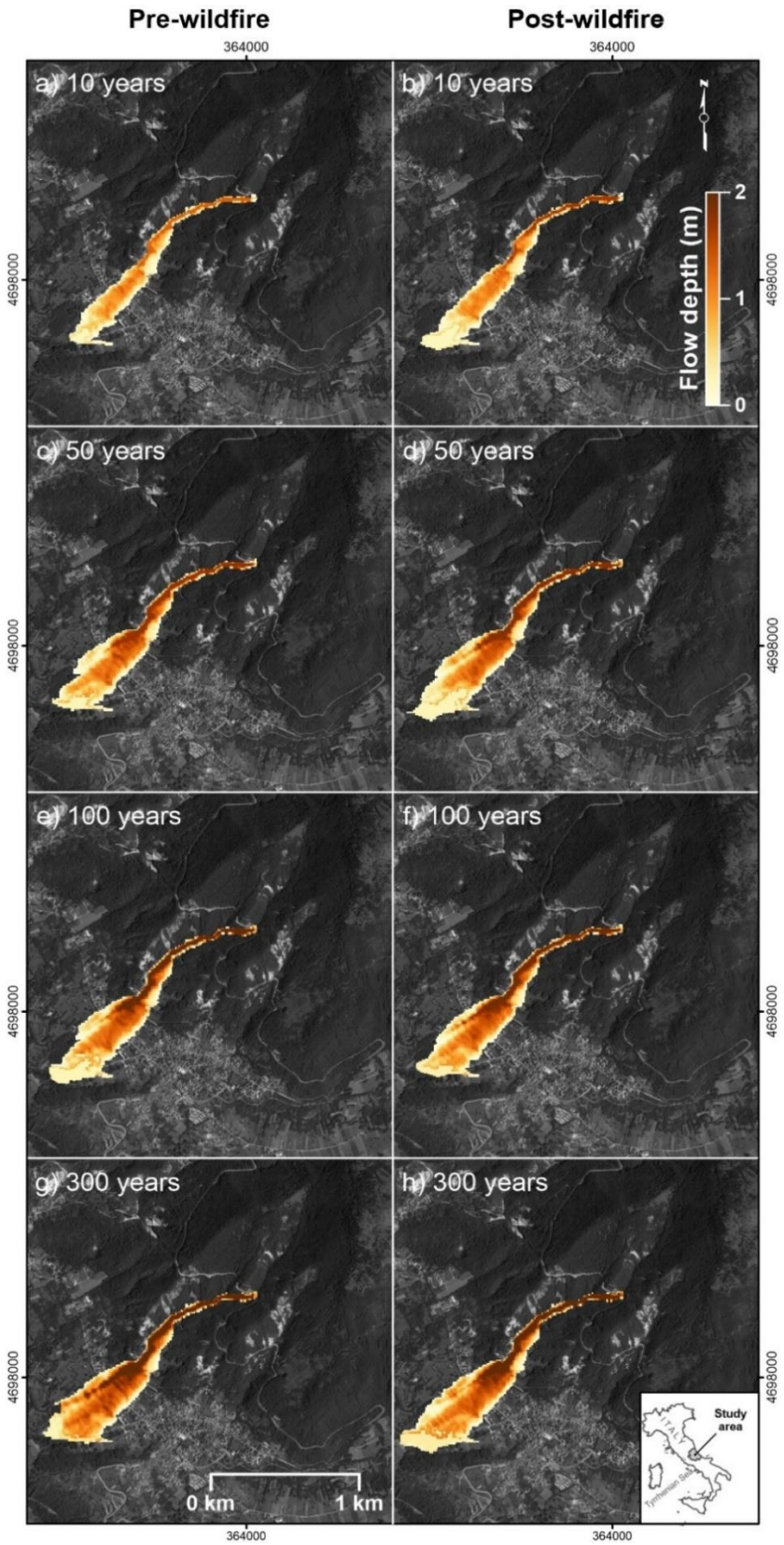

Figure 8 - Pre- and post-wildfire flow depth inundation scenarios derived from 2D hydrodynamic modeling.

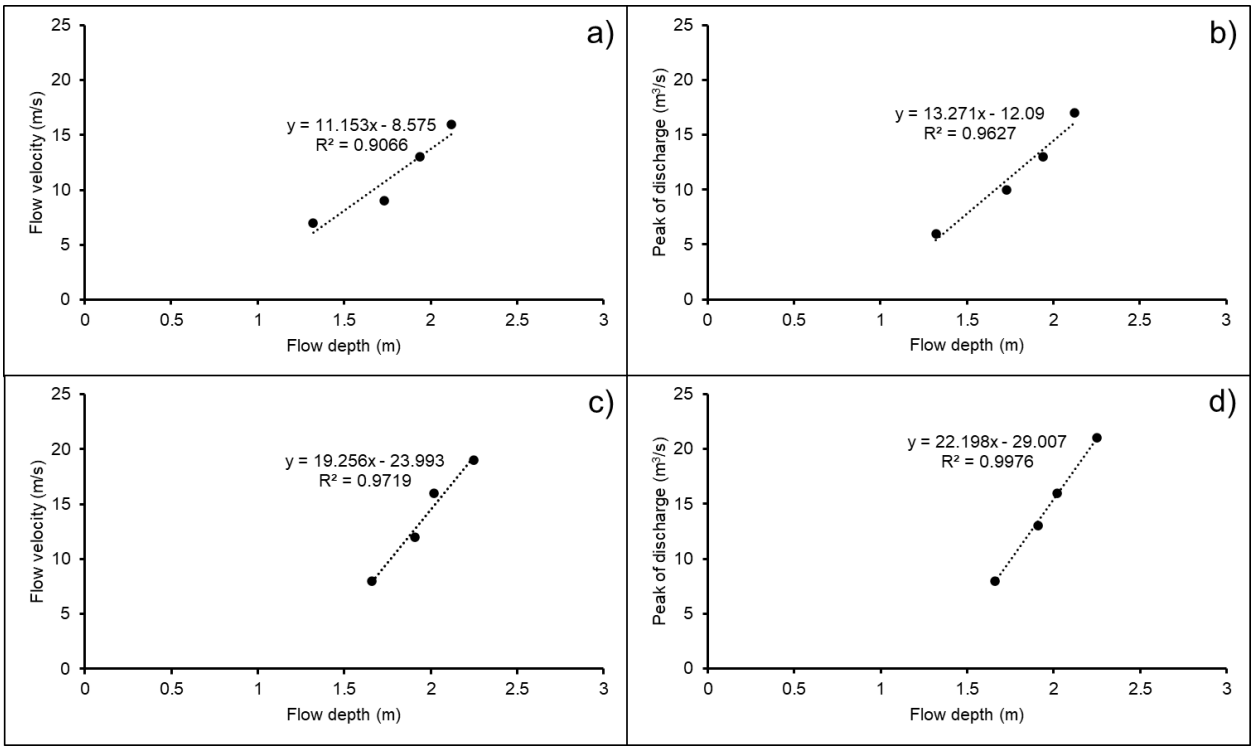

404

405 *Figure 9 – Graphs showing correlation between flow depth and flow velocity in pre- and post-wildfire conditions (a and c,*
406 *respectively) and flow depth and peak of discharge in pre- and post-fire conditions (b and d, respectively).*

Figure 10 – Photographs showing flow erosional signature on tree stems (i.e. thickness) after the August 24 event. Pictures are taken along the Fosso delle Pescine channel, below the headwater catchment. In this segment of the channel flow thickness reached a maximum height of ~120 cm.

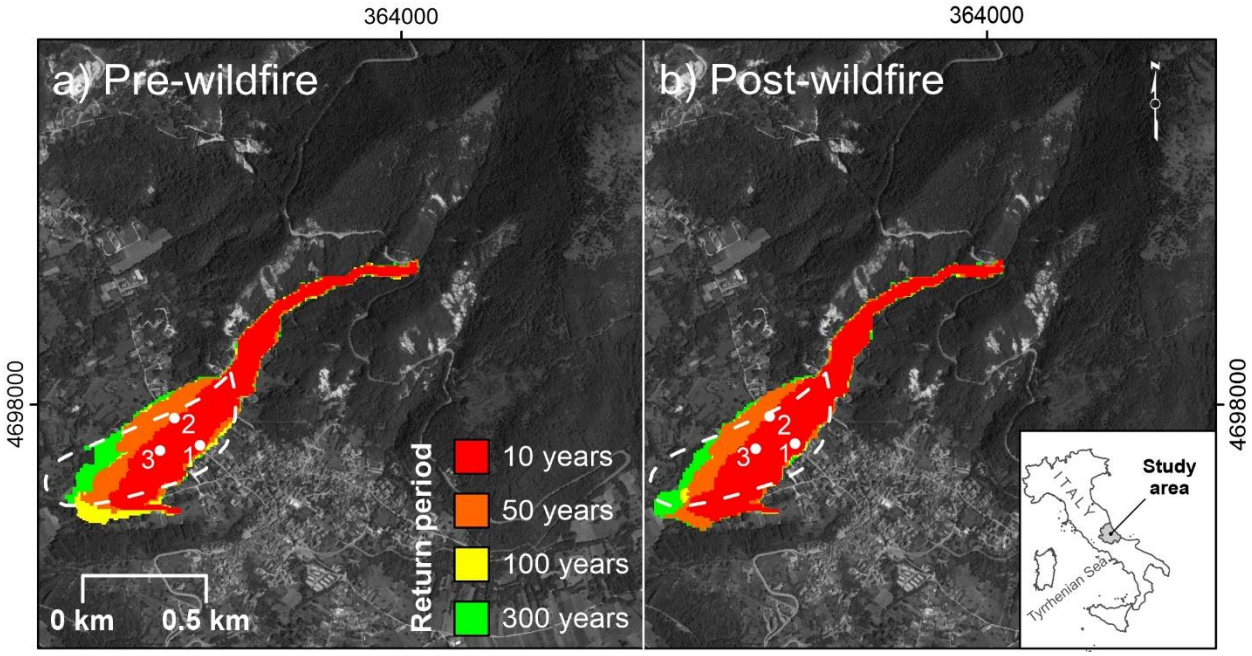

411

412 *Figure 11 – Debris flow/flood hazard maps of the Fosso delle Pescine catchment and locations of photographs of the 2020 event*
413 *of Figure 1.*

414 **5.0 Conclusions**

415 The analysis of the debris flow/flood hazard in the *Fosso delle Pescine* catchment indicates that
416 significant events can affect the western portion of the Arischia village in the L'Aquila municipality of
417 central Italy. Hazard models' reconstruction was carried out through a reduced complexity approach
418 based on the overlay of multiple inundation scenarios derived by 2D hydrodynamic modeling of a non-
419 Newtonian equivalent fluid. Input hydrographs for different return period were reconstructed on the basis
420 of the reconstructed IDF curves and considering a sediment concentration of 50 %, which represent a
421 transition condition between debris floods induced by debris flow dilution and debris flows. Bingham
422 fluid parameterization was completed considering this process combination and available sediment
423 characteristics. Sediment availability at the headwater was estimated through field measures indicating a
424 budget able to trigger only high frequency debris flow events. In case of lower frequency rainfall events,
425 lower concentration sediment laden flow (e.g. hyperconcentrated flow) can be developed. The adopted
426 reduced complexity modeling approach that considers modeling parameter at transition between debris-
427 flow and -flood would make inundation scenarios better representative of the event occurred in August
428 2020, that exhibits a combination of flow conditions (from debris flow to flood).

429 Results of simulation have been validated through the comparison and debris flow/flood depth and extent
430 of the phenomenon. Depth was extracted from filed survey of the external morphology of trees impacted
431 by debris flows/flood. Extent of potential areas affected by debris flow/flood was determined using
432 photographs location of 2020 event and the extent of debris fan reported in the available geological map.
433 A good correspondence between simulations results and data gathered from field surveys and geological
434 maps have been found, proving the reliability of the proposed approach.

435 The new reduced complexity method proposed in this research accounts for initiation and propagation
436 through shallow water equation based approach, resulting easy to be used and potentially applicable in

wide range of case study worldwide. This represents a great advantage in those case when it is not possible to retrieve all the information needed for more complex types of analyses.

In fact, the approach has proved that can be applied for fast assessment of debris flow/flood hazard in both pre- and post-wildfire conditions, also in absence of all of the needed constraints. In comparison to existing methods, it is flexible and capable of reliable estimation accounting for a certain degree of safety in huma life protection perspective. In addition, although of reduced-complexity, the method is based on a fully deterministic propagation simulation that might ensure consistency of simulations at variating debris flow/flood volume. Finally, the development of the model on the basis of multiple return periods (10, 50, 100 and 300 years) debris flow inundation scenarios might represent a new hazard model reconstruction criterion, which do not account for flow thickness and it is able to represent all of the hazard classes, maintaining their statistical significance.

Declarations

Conflicts of interests: The authors have no conflicts of interest to declare. All co-authors have seen and agree with the contents of the manuscript.

References

Borga, M., et al. (2014). Hydrogeomorphic response to extreme rainfall in headwater systems: flash floods and debris flows. Journal of Hydrology, 518, 194–205. https://doi.org/10.1016/j.jhydrol.2014.05.022

Calcaterra, D., et al. (2007). Relations between fire, vegetation and landslides in the heavily populated metropolitan area of Naples, Italy. In Schaefer, V. R., Schuster, R. L., and Turner, A. K. (Eds.), Proceedings of the 1st North American Landslide Conference (pp. 1448–1461). Denver, CO, USA: Association of Environmental & Engineering Geologists.

Cannon, S. H. (2001). Debris-flow generation from recently burned watersheds. Environmental and Engineering Geoscience, 7, 321–341.

Cannon, S. H., et al. (2010). Predicting the probability and volume of postwildfire debris flows in the intermountain western United States. Bull. Geol. Soc. Am., 122(1-2), 127–14446(2).

Cannon, S. H., and DeGraff, J. V. (2009). The increasing wildfire and post-fire debris-flow threat in Western USA, and implications for consequences of climate change. In Sassa, K., and Canuti, P. (Eds.), Landslides - disaster risk reduction (pp. 177-190). Berlin, Germany: Springer.

Carabella, C., Miccadei, E., Paglia, G., and Sciarra, N. (2019). Post-wildfire landslide hazard assessment: the case of the 2017 Montagna del Morrone fire (Central Apennines, Italy). Geosciences, 9(4), 175. https://doi.org/10.3390/geosciences9040175

Church, M., and Jakob, M. (2020). What is a debris flood? Water Resour Res, 56(8). https://doi.org/10.1029/2020WR027144

Dong, Y. (2009). The role of sediment budget in understanding debris flow susceptibility. Earth Surface Processes and Landforms, 34(12), 1612-1624. https://doi.org/10.1002/esp.1850

Gabet, E. J., and Bookter, M. (2008). A morphometric analysis of gullies scoured by postfire progressively bulked debris flows in southwest Montana, USA. Geomorphology, 96, 298-309. https://doi.org/10.1016/j.geomorph.2007.03.016

Iverson, R. M. (2000). Landslide triggering by rain infiltration. Water Resources Research, 36(7), 1897-1910. https://doi.org/10.1029/2000WR900090

Kean, J. W., Staley, D. M., and Cannon, S. H. (2011). In situ measurements of post-fire debris flows in southern California: Comparisons of the timing and magnitude of 24 debris-flow events with rainfall and soil moisture conditions. Journal of Geophysical Research, 116, F03025. https://doi.org/10.1029/2011JF002005

Key, C., & Benson, D. (2006). Landscape assessment: ground measure of severity, the Composite Burn Index; and remote sensing of severity, the Normalized Burn Ratio. In DC Lutes, RE Keane, JF Caratti, CH Key, NC Benson, S Sutherland, & LJ Gangi (Eds.), FIREMON: Fire Effects Monitoring and Inventory System (pp. LA1-51). USDA Forest Service, Rocky Mountain Research Station, General Technical Report RMRS-GTR-164-CD, Ogden, UT.

Miller, J. D., & Thode, A. E. (2007). Quantifying burn severity in a heterogeneous landscape with a relative version of the delta Normalized Burn Ratio (dNBR). Remote Sensing of Environment, 109(1), 66-80.

Moody, J. A., & Martin, K. J. (2001). Initial hydrologic and geomorphic response following a wildfire in the Colorado Front Range. Earth Surface Processes and Landforms, 26, 1049-1070.

Parise, M., & Cannon, S. H. (2012). Wildfire impacts on the processes that generate debris flows in burned watersheds. Natural Hazards, 61, 217-227. https://doi.org/10.1007/s11069-011-9769-9

Pierson, T. C., & Costa, J. E. (1987). A rheologic classification of subaerial sediment-water flows. In J. E. Costa & G. F. Wieczorek (Eds.), Debris flows/avalanches: Processes, recognition, and mitigation. Geological Society of America, Reviews in Engineering Geology, 7, 1-12.

Roy, D. P., Boschetti, L., & Trigg, S. N. (2006). Remote sensing of fire severity: Assessing the performance of the Normalized Burn Ratio. IEEE Transactions on Geoscience and Remote Sensing, 44(4), 112-116. https://doi.org/10.1109/LGRS.2005.858485

Santi, P. M., deWolfe, V. G., Higgins, J. D., Cannon, S. H., & Gartner, J. E. (2008). Sources of debris flow material in burned areas. Geomorphology, 96(3-4), 310-321. https://doi.org/10.1016/j.geomorph.2007.02.022

Santo, A., Ascione, A., Di Crescenzo, G., Miccadei, E., Piacentini, T., & Valente, E. (2013). Tectonic-geomorphological map of the middle Aterno River valley (Abruzzo, Central Italy). Journal of Maps, 10(3), 365-378. https://doi.org/10.1080/17445647.2013.867545

Staley, D. M., Kean, J. W., & Rengers, F. K. (2020). The recurrence interval of post-fire debris-flow generating rainfall in the southwestern United States. Geomorphology, 359, 107163. https://doi.org/10.1016/j.geomorph.2020.107392

Staley, D.M., Kean, J.W., Cannon, S.H., Schmidt, K.M., Laber, J.L. (2013). Objective definition of rainfall intensity-duration thresholds for the initiation of post-fire debris flows in southern California. Landslides. 10(5), 547–562. https://doi.org/10.1007/s10346-012-0341-9

513 Westerling, A.L., Bryant, B.P. (2008). Climate change and wildfire in California. Climatic Change. 87,
514 s231-s249. https://doi.org/10.1007/s10584-007-9363-z

515 Wieczorek, G.F. et al. (2001). Debris-flow and flooding hazards associated with the December 1999
516 storm in coastal Venezuela and strategies for mitigation. USGS Open File Report No. 2001–2144.

517 Williams, A.P. et al. (2019). Observed impacts of anthropogenic climate change on wildfire in California.
518 Earth's Future. 7(8), 892–910. https://doi.org/10.1029/2019EF001210